Bounded error detection of the wind gusts effect on a small-scaled helicopter

Walid Achour * **Hélène Piet-Lahanier** *
Houria Siguerdidjane **

* *Office National d'Etudes et de Recherches Aérospatiales (ONERA), France, walid.achour@onera.fr, Helene.Piet-Lahanier@onera.fr*
** *École Supérieure d'Électricité (SUPELEC), France, Houria.Siguerdidjane@supelec.fr*

Abstract This paper deals with the problem of estimating the effects of wind gusts on a small helicopter type UAV. A model of the UAV is first described, including potential effects of wind. Identification of the state vector representing the UAV is performed using a set estimation technique in order to characterize the variation boundaries of the flight induced by the presence of wind. Simulation results are presented to illustrate the detection performance.

Keywords: Helicopter modeling , bounding approach state estimation, atmospheric turbulence detection.

1. INTRODUCTION

Unmanned aerial vehicles (UAV) have been sought for a wide range of applications such as surface and utilities inspection, search and rescue operations, air pollution monitoring and environmental surveillance. However, in the case of small UAV's, the flight domain is rapidly affected by atmospheric turbulence. Hence, disturbances such as wind gusts have a very significant nonlinear effect on the expected performance of the guidance and autopilot loop and therefore strongly affect the feasibility of the mission. In most descriptions of guidance loop synthesis for these vehicles, such an impact has not been taken into account. This contribution consists of describing a procedure to detect the effect of aerological disturbances on a small helicopter-type UAV so that the guidance loop could take this effect into account. The paper is organised as follows. We first describe the UAV and its dynamical model. The estimation procedure, based on the use of set-membership approach, is presented and the main steps of the algorithm are described. A simulated example is used to illustrate the obtained results.

1.1 UAV description

The UAV considered in this paper is a VARIO Benzin-Acrobatic. The vehicle is powered by a 23 cm^3 Zenoah engine connected through a shaft to the main rotor blades of diameter 1.80 m. Its nominal weight is 6.5 kg for the commercial version. Figure 1 presents the vehicle used for experimental purposes by the ONERA DCSD team in Toulouse. This helicopter has been equipped with several sensors including an IMU and a GPS.

1.2 Dynamic equations

The dynamics of the helicopter are modelled using a conventional six degree of freedom rigid body model driven by forces and moments that explicitly include the effects of the main and tail rotors.

Figure 1. Vario helicopter

Let $\zeta = (x\ y\ z)^t$ denote the relative position vector of the helicopter regarding the inertial frame $(\mathcal{I})$. The velocity of the center of mass expressed in the inertial frame is denoted by $v = \dot{\zeta}$. Let m be the total mass, $I = diag(I_1, I_2, I_3)$ be the diagonal matrix representing the inertia of the helicopter and $(e_1\ e_2\ e_3)$ be a canonical basis of R^3. The vector $\Omega = (p\ q\ r)^t$ is the angular velocity of the vehicle in the body fixed frame $(\mathcal{B})$.
Let $R : (\mathcal{B}) \rightarrow (\mathcal{I})$ denote the rotation matrix representing the orientation of the body fixed frame $(\mathcal{B})$, where $\mathcal{R} \in SO(3)$ is an orthogonal matrix defined by :

$$\mathcal{R} = \begin{pmatrix} c_\theta c_\psi & s_\psi s_\theta c_\phi - c_\psi s_\phi & c_\psi s_\theta c_\phi + s_\psi s_\phi \\ c_\theta s_\psi & s_\psi s_\theta s_\phi + c_\psi c_\phi & c_\psi s_\theta s_\phi - s_\psi c_\phi \\ -s_\theta & c_\theta s_\phi & c_\theta c_\phi \end{pmatrix} \quad (1)$$

where $c_\alpha = \cos\alpha$, $s_\alpha = \sin\alpha$ and (ϕ, θ, ψ) represent the Euler angles.
The dynamic evolution of $\mathcal{R}$ is given by (Murray et al.

(1994)):

$$\dot{\mathcal{R}} = \mathcal{R}\Omega_\times$$

where

$$\Omega_\times = \begin{pmatrix} 0 & -r & q \\ r & 0 & -p \\ -q & p & 0 \end{pmatrix}$$

is the skew symmetric matrix such that $\Omega_\times u = \Omega \times u$

Using the Newton-Euler formalism, the dynamical equations of the helicopter motion are written as:

$$\begin{cases} \dot{\zeta} = v \\ m\dot{v} = \mathcal{F} + \mathcal{F}_{wind} \\ \dot{\mathcal{R}} = \mathcal{R}\Omega_\times \\ I\dot{\Omega} = -\Omega \wedge I\Omega + \mathcal{M} + \mathcal{M}_{wind} \end{cases} \tag{2}$$

where $\mathcal{F}$ is the resulting external force acting on the helicopter and $\mathcal{M}$ is the resulting external torque applied to the helicopter at the center of mass, without wind. The terms $\mathcal{F}_{wind}$ and $\mathcal{M}_{wind}$ represent the force and torque due to the effect of the wind gusts respectively. The following paragraph describes the explicit expression of these terms.

Resulting force $\mathcal{F}$: The different forces acting on the system are

- the thrust of the propellers F_p,
- the weight mge_3
- the aerodynamic force of the fuselage F_f.

The thrust of the propellers F_p results from the main rotor thrust F_{mr} and the tail rotor thrust F_{tr}. The resulting force $\mathcal{F}$ is then obtained as

$$\mathcal{F} = mge_3 + \mathcal{R}.(F_{mr} + F_{tr} + F_f) \tag{3}$$

The main rotor dynamics play a major role in terms of its contribution to the dynamics of the helicopter flight.

In the following, we assume that the three assumptions below are satisfied (Gavrilets et al. (2001)):

- the vertical flapping angle 'β' is assumed to remain very small,
- the angle of attack of each blade is small,
- the angular accelerations are negligible compared to the angular rate of turn multiplied by the rotation speed.

Under these assumptions, the longitudinal and lateral blade flapping dynamics a_1 and b_1 can be modeled by the two following coupled first-order differential equations:

$$\begin{cases} \tau_f \dot{a}_1 + a_1 = -\tau_f q + \dfrac{8}{\gamma\Omega^2}\dfrac{k_\beta}{I_\beta} b_1 + K_{lon}(\delta_{lon} + K_c c_1) \\ \tau_f \dot{b}_1 + b_1 = -\tau_f p + \dfrac{8}{\gamma\Omega^2}\dfrac{k_\beta}{I_\beta} a_1 + K_{lat}(\delta_{lat} + K_d d_1) \end{cases} \tag{4}$$

where γ is the Lock number, k_β is the rotor solidity ratio, I_β is the blade moment of inertia about the flapping hinge and τ_f is the effective rotor time constant ($\tau_f > 0$). K_{lon} and K_{lat} are the effective steady-state longitudinal and lateral gains from inputs to main rotor flap angles, scheduled with main rotor speed; δ_{lon} and δ_{lat} are the longitudinal and lateral control inputs; c_1 and d_1 are the longitudinal and lateral stabilizer Bell bar states respectively. The dynamic equations can be written as (Gavrilets et al. (2001)):

$$\begin{cases} \tau_s \dot{c}_1 + c_1 = -\tau_s q + C_{lon}\delta_{lon} \\ \tau_s \dot{d}_1 + d_1 = -\tau_s p + D_{lat}\delta_{lat} \end{cases} \tag{5}$$

C_{lon} and D_{lat} are the effective steady-state longitudinal and lateral gains from the inputs to the Bell bar flap angles and τ_s is the stabilizer bar's time ($\tau_s > 0$).

Assuming that the longitudinal and lateral flapping angles a_1 and b_1 are small, the total thrust of the main rotor F_{mr} can be approximated by:

$$F_{mr} \approx |F| \begin{pmatrix} -a_1 \\ b_1 \\ -1 \end{pmatrix} \tag{6}$$

where F is the norm of the thrust generated by the main rotor:

$$F = mg + K_z(\delta_{col} - \delta_{sta})$$

K_z can be experimentally obtained as the ratio between the vertical acceleration and the control value δ_{col} and δ_{sta} is the control value in stationary hovering flight condition.

Tail rotor dynamics : The tail rotor thrust representation does not take into account complex interactions between the main and tail rotors. As in Gavrilets et al. (2001) the thrust is expressed as being proportional to the lift of the tail rotor and the control yaw.

$$F_{tr} = (0 \ K_{ped}\delta_{ped} \ 0)^t \tag{7}$$

where δ_{ped} is the control input and K_{ped} is constant ($K_{ped} > 0$).

Fuselage force F_f: The fuselage force mostly originates from air drag. The drag force is defined along the body coordinate system axes and is assumed to act on the body and thus creates no torque. It can be approximated by (Gavrilets (2003)):

$$F_f = -\frac{1}{2}\rho \begin{pmatrix} c_f^x S_f^x V_\infty u_a \\ c_f^y S_f^y V_\infty v_a \\ c_f^z S_f^z V_\infty (w_a + w_{in}) \end{pmatrix} \tag{8}$$

where S_f^x, S_f^y, S_f^z are the effective drag areas of the fuselage in x_b, y_b and z_b directions; c_f^x, c_f^y and c_f^z are the drag, lateral and lift coefficients respectively; the velocity V_∞ is defined as follows:

$$V_\infty = (u_a^2 + v_a^2 + (w_a + w_{in})^2)^{1/2}$$

where $(u_a, v_a, w_a)^t$ is defined as the difference between the velocity of the vehicle expressed in the body frame ($\mathcal{B}$) and the wind velocity ($u_a = u - u_w$; $v_a = v - v_w$; $w_a = w - w_w$); w_{in} is the induced velocity in hover flight condition whose formula is given by:

$$w_{in} = \sqrt{\frac{mg}{2\rho\pi R_{mr}^2}}$$

R_{mr} is the main rotor radius.

Resulting torque $\mathcal{M}$: The resulting torque created by the various forces can be represented by the expression:

$$\mathcal{M} = b_{mr} \wedge F_{mr} + b_{tr} \wedge F_{tr} + \Delta_k \tag{9}$$

where b_{mr} and b_{tr} are the moment arm of the main and tail rotors respectively; Δ_k is the roll moment corresponding

to the spring effect of the rotor hub (Mahony et al. (1999)). This term may be expressed as

$$\Delta_k = k_\beta \left(b_1 \ a_1 \ 0\right)^t$$

Effects of wind gusts: First the wind gust model will be described. The corresponding force $\mathcal{F}_{wind}$ and torque $\mathcal{M}_{wind}$ acting on the helicopter will be detailed afterwards.

Wind gust model: The mathematical model of wind gusts is a simple first-order model.

- Wind gust component along the x-axis:

$$\begin{cases} u_w = 0 & \text{for } x < x_{sg} \\ u_w = \dfrac{u_m}{2}(1 - \cos(\pi x / L_u)) & \text{for } x_{sg} < x < x_{eg} \\ u_w = 0 & \text{for } x_{eg} < x \end{cases} \quad (10)$$

- Wind gust component along the y-axis:

$$\begin{cases} v_w = 0 & \text{for } x < x_{sg} \\ v_w = \dfrac{v_m}{2}(1 - \cos(\pi x / L_u)) & \text{for } x_{sg} < x < x_{eg} \\ v_w = 0 & \text{for } x_{eg} < x \end{cases} \quad (11)$$

- Wind gust component along the z-axis:

$$w_w = 0 \quad (12)$$

- Wind gust velocity norm:

$$V_w = \sqrt{u_w^2 + v_w^2 + w_w^2} \quad (13)$$

where x_{sg} and x_{eg} are respectively the distance between the helicopter location and the gust origin location before entering it and the distance between the helicopter location and the gust origin location after leaving it. L_u is the half length of the gust. The values u_m and v_m are the densities of the gust velocity.

Resulting force $\mathcal{F}_{wind}$ and torque $\mathcal{M}_{wind}$: In this section, we consider the effect of a lateral wind gust. This lateral perturbation acting on the fuselage causes a drag force F_f^w along the x and y body axes of the helicopter and a torque that is assumed negligible:

$$F_f^w = -\frac{1}{2}\rho \begin{pmatrix} c_x^w S_f^x V_w u_w \\ c_y^w S_f^y V_w v_w \\ 0 \end{pmatrix}$$

where c_x^w and c_y^w are the aerodynamics coefficients. The presence of a wind gust creates a destabilizing roll effect on the main rotor (Prouty (1990)) which is modeled as a torque M_{mr}^w about the axe x_b:

$$M_{mr}^w = \left(\frac{1}{4k_\beta}\rho S_{mr} c_{mr}^w R_{mr} \dot{\gamma} V_w \sqrt{(0.75R_{mr})^2 + b_{mr}^2} \ 0 \ 0\right)^t$$

where S_{mr} is the area of the main rotor disk; c_{mr}^w is the thrust coefficient; γ is the azimuth angle of the main rotor blades.

The gust also creates disturbances on the tail rotor which are summarized as a force F_{tr}^w

$$F_{tr}^w = \left(0 \ 4\rho\pi R_{tr}^2 V_w v_w \ 0\right)^t$$

and a torque M_{tr}^w

$$M_{tr}^w = b_{tr} \wedge F_{tr}^w$$

Thus, the resulting force and torque in the presence of wind gust are:

$$\mathcal{F}_{wind} = \mathcal{R}.(F_f^w + F_{tr}^w) \quad (14)$$

$$\mathcal{M}_{wind} = M_{mr}^w + M_{tr}^w \quad (15)$$

2. ESTIMATION OF THE WIND GUST EFFECT

The aim of the detection method is not to exactly characterize the aerological perturbation but to evaluate if they have a global effect on the flight ability of the vehicle. This is why we are not looking for a single point estimate corresponding to the mean value evolution but for a characterization of the boundaries variation of perturbations. Set estimation is therefore a well-suited technique for that purpose.

2.1 Ellipsoidal state estimation

We consider a dynamic discrete state space evolution of the form

$$\begin{cases} X_{k+1} = A_k X_k + B_k u_k + w_k \\ z_{k+1} = F_k X_k + v_k \end{cases} \quad (16)$$

In the following, we make the assumption that the state perturbations and noise measurements are unknown but bounded without additional underlying probabilistic assumptions. We are therefore seeking the set of all values of the state vector that are consistent with this hypothesis in the sense that all errors fall within specified known bounds. The set of perturbations and noise bounds are expressed as

$$w_k^t W_k^{-1} w_k \leq 1$$
$$v_k^t V_k^{-1} v_k \leq 1$$

where W_k and V_k are given matrices. This approach corresponds to guaranteed estimation that was initially introduced by Schweppe (1968) and by Bertsekas and Rhodes (1971). Several methods have been developed to define the boundary of this set or to compute a set guaranteed to contain it. The main approaches compute the approximate set under the form of an ellipsoid, but other methods have been described that result in characterizing a polyhedral boundary or determine the union of intervals to which all state vectors belong (for example Milanese et al. (1996) for an overview).

The approach used in this work is based on the extension of the single-cut ellipsoid algorithm (Pronzato and Walter (1994)) initially designed for parameter estimation for state estimation problems as described in Maksarov and Norton (2002).

The initial phase of the algorithm defines an ellipsoid that is assumed to contain all values of the initial state vector X_0. The ellipsoid is characterized by its center $\hat{X}_0$ and its associated matrix P_0 that defines its main axes and amplitude.
The estimation method is based on two steps very similar to those of Kalman filtering.
First, one produces a predicted ellipsoid on a given time horizon. This prediction set is centered at the predicted ellipsoid center, $\hat{X}_{k/k+1} = A_k X_k + B_k u_k$. Updates of the associated matrix must take into account the assumed state

perturbations. We operate n_w successive modifications (n_w being the dimension of the state perturbation vector w), of the ellipsoid, each corresponding to the uncertainty modification due to one process noise component. This procedure is suboptimal for non scalar perturbations but proves to be computationally efficient. Moreover, the perturbations are assumed to belong to an orthotope whose equations are:

$$W_k = \bigcap_i \{w_k : -b_i \leq c_i^t w_k \leq b_i\}$$

where b_i is the bound associated with the eigenvector c_i of W_k. The initial ellipsoid matrix $P^0_{k/k-1}$ is obtained as $A_k P_k A_k^t$. In addition, each modification operates the transformation:

$$P^i_{k/k-1} = (1+\rho_i)P^{i-1}_{k/k-1} + (1+\rho_i^{-1})b_i^2 G_k c_i c_i^t G_k^t \quad (17)$$
$$i = 0, ..., l-1$$

where the value of ρ is the positive root of

$$n\rho_i^2 + (n-1)a_i\rho_i - a_i = 0 \quad (18)$$

where $a_i = b_i^2 c_i^t G_k^t (P^{i-1}_{k_k-1})^{-1} G_k c_i$ and n is the state dimension.

Finally $P_{k/k-1} = P^l_{k/k-1}$.

When the prediction step has been realized, an update of the estimated set is performed by taking a new measurement into account. We first seek whether the predicted model error satisfies the assumption on the measurement outer bounds. We compute the normalized distance from the ellipsoid center to the new bounds by

$$\alpha = \frac{e_k^t V_k^{-1} e_k - \sqrt{e_k^t V_k^{-1} e_k}}{\sqrt{h_k^t P_{k/k-1} h_k}} \quad (19)$$

where e_k is the innovation ($e_k = y_k - F_k \hat{X}_{k/k+1}$) and h_k is the normal to the approximating hyperplane ($h_k = F_k^t V_k^{-1} e_k$).

If α is greater than 1, the intersection is empty and a specific procedure must be defined. If α is lower or equal to $-1/n$, the measurement does not carry any additional information and no update is required. In other cases, the state space estimated set must be updated. Define

$$\tau_k = \frac{1+n\alpha}{1+n}; \sigma_k = \frac{2\tau_k}{(1+\alpha)}; \beta_k = \frac{n^2(1-\alpha^2)}{n^2-1}$$

The ellipsoid center $\hat{X}_k$ is obtained as:

$$\hat{X}_k = \hat{X}_{k/k-1} + \tau_k \frac{P_{k/k-1} h_k}{\sqrt{h_k^t P_{k/k-1} h_k}} \quad (20)$$

and the symmetric definite positive matrix defining its shape is

$$P_k = \beta_k (P_{k/k-1} - \sigma_k \frac{P_{k/k-1} h_k h_k^t P_{k/k-1}}{h_k^t P_{k/k-1} h_k}) \quad (21)$$

It remains to define the procedure when the intersection is considered empty. The method implemented in the simulation operates a translation of the resulting ellipsoid toward the measurement image, halfway to the exact measurement image. This is of importance as the detection of aerological perturbations will be operated on the basis of a lack of consistency between predicted outputs and real measurements.

2.2 Detection of aerological perturbations

Our detection process of aerological disturbance is performed by comparing the prediction wind-free model to the measurements and thus deciding whether wind gusts react with the helicopter flight.

Choice of identification model: The model used for identification purpose is described by equation (22). It corresponds to the case where there is no aerological effect on the vehicle.

$$\begin{cases} \dot{\zeta} = v \\ m\dot{v} = \mathcal{F} \\ \dot{\mathcal{R}} = \mathcal{R}\Omega_\times \\ I\dot{\Omega} = -\Omega \wedge I\Omega + \mathcal{M} \end{cases} \quad (22)$$

Measurement vector: The measurement vector y_m includes the sensor outputs, i. e., altitude (m), velocity (m/sec), Euler angles (deg), and angular velocity (rad/sec). The vector y_m is therefore defined by:

$$y_m = (x, y, z, v_x, v_y, v_z, \phi, \theta, \psi, p, q, r)^t$$

The unmeasured states a_1, b_1,c_1 and d_1 are estimated.

2.3 Simulation results

In this section, simulation results are presented to illustrate the ability of the bounded-error state estimation algorithm to detect the aerological disturbances. On each graphic, the curve ($-$) represents the predicted value without wind disturbance, the curve ($-.-$) corresponds to the ellipsoid center evolution, and the curve (..) shows the boundary values of the estimated ellipsoid.

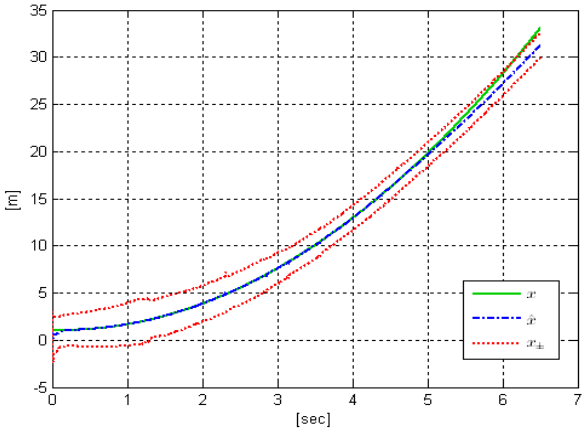

Figure 2. Evolution of predicted and estimated x position

The evolution of the position and velocity components are represented in Figures 2 - 3, and in Figures 4-5 respectively. The roll and yaw are exhibited in Figures 6-7 and the components of the angular velocities on Figures 8-9.
We can detect the impact of the lateral wind gust in the evolution of the position and the velocity in the x-y directions, and in the evolutions of roll, yaw, p and r. Note that the position z, velocity v_z, pitch θ and angular velocity q are not represented as the influence of aerological perturbation is very low. In this example, ellipsoidal bounding technique provides a suitable detection of longitudinal and lateral flapping angles and stabiliser bar Bell

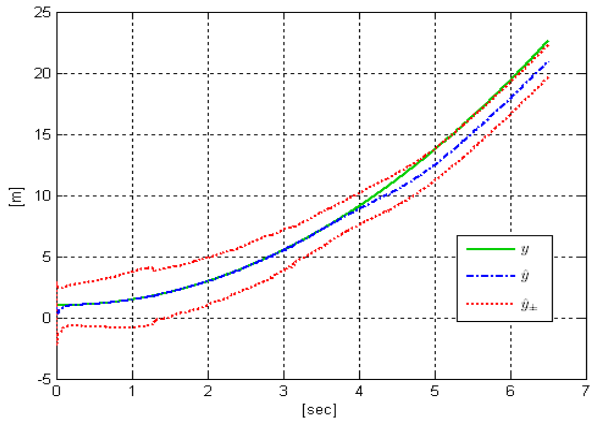

Figure 3. Evolution of predicted and estimated y position

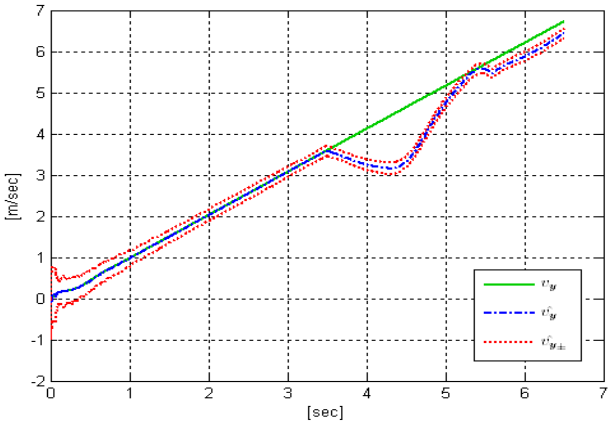

Figure 5. Evolution of predicted and estimated v_y velocity

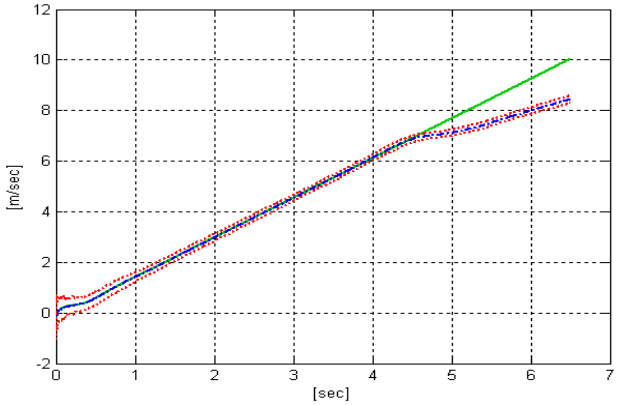

Figure 4. Evolution of predicted and estimated v_x velocity

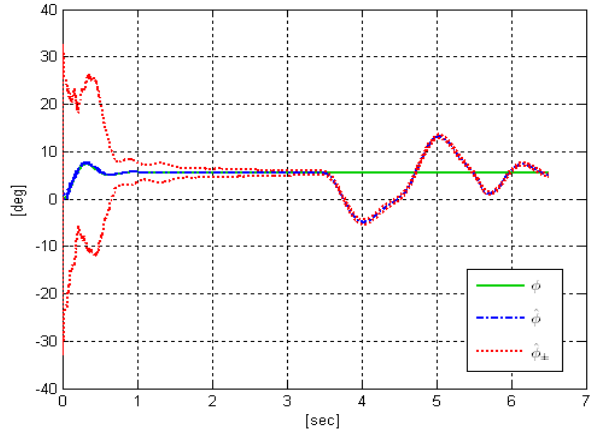

Figure 6. Evolution of predicted and estimated ϕ angle

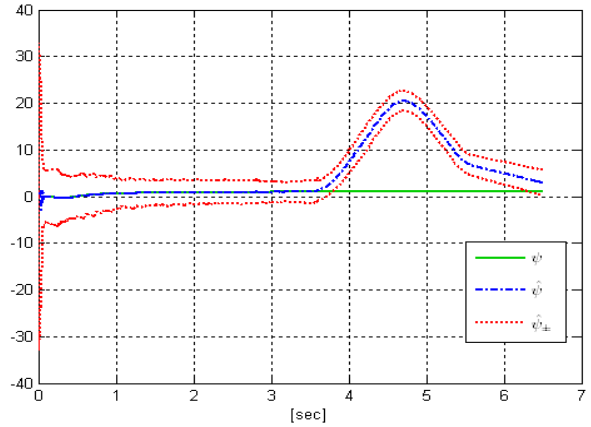

Figure 7. Evolution of predicted and estimated ψ angle

observe that, before wind gust, the estimates converge to the "real" dynamical states. When a wind gust occurs, there is no longer consistency between predicted outputs and measurements for the set of values that are affected by the wind effect. The procedure described above to modify the ellipsoid when the measurements and predicted outputs are not consistent allows the tracking of the effect of the aerological perturbation.
These results are of preliminary nature as it remains to be investigated their sensitivity to the hypothesis on the perturbation and noise bounds and to the reliability of the dynamical model.

3. CONCLUSION

In this paper, we have presented a method for detecting the effect of aerological perturbations on the flight performance of a small helicopter-like UAV. A model including a representation of the forces and torques induced by the presence of wind and aerological perturbations has been described. Identification procedure based on ellipsoidal characterization of the state vector variations has been applied on a simulated example of a UAV trajectory which is subjected to the influence of a wind gust after several seconds of wind-free flight. From the obtained results, it can be pointed out that it is possible to determine the time when there is no longer consistency between wind-free hypothesis and measurements and therefore to conclude on the presence of aerological effects. It remains to be studied the robustness of the resulting detection to both perturbation and noise bounds hypothesis and to the reliability of the model. Experimental work will be planned in the near future by using the Vario vehicle in the gust generator of the experimental area in ONERA. The final step is to define a suitable guidance law that modifies the UAV

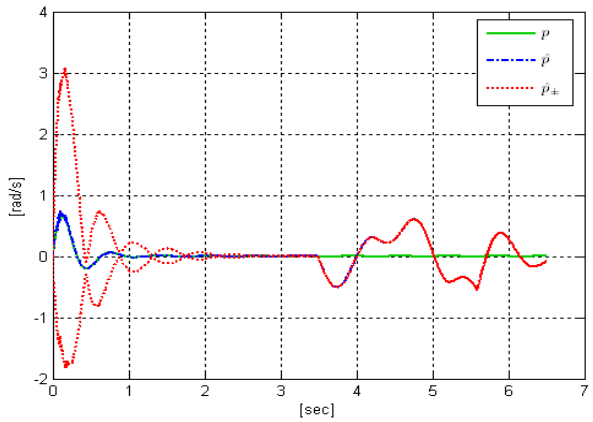

Figure 8. Evolution of predicted and estimated angular velocity p

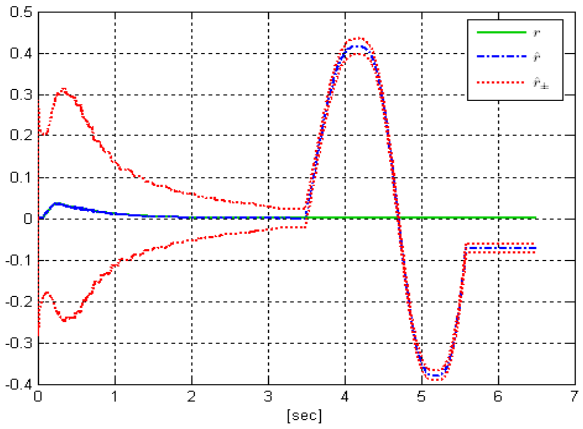

Figure 9. Evolution of predicted and estimated angular velocity r

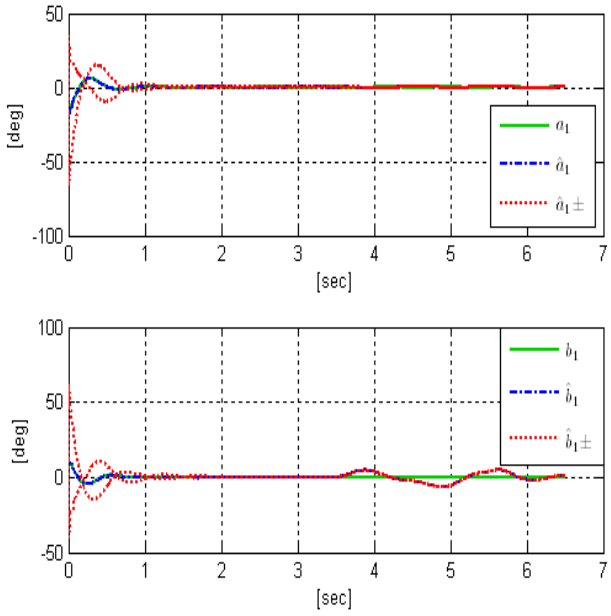

Figure 10. Evolution of predicted and estimated longitudinal and lateral blade flapping a_1,b_1

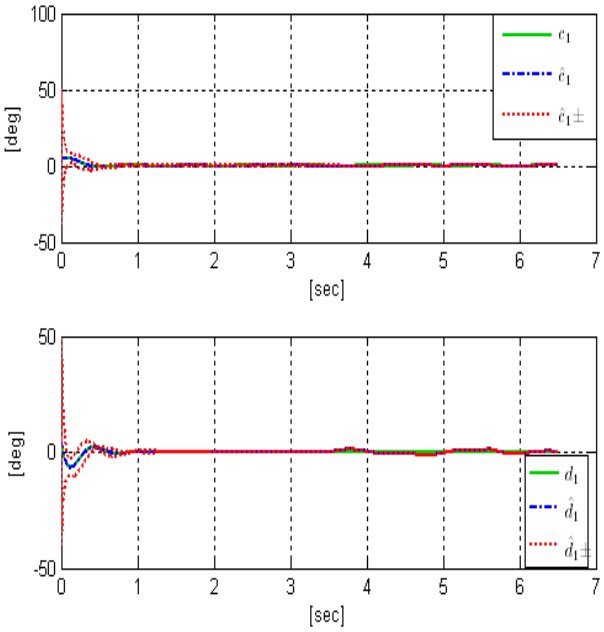

Figure 11. Evolution of predicted and estimated longitudinal and lateral stabilizer bar Bell c_1,d_1

trajectory whenever aerological effects are detected in order to satisfy both mission and security requirements.

REFERENCES

Bertsekas, D. and Rhodes, I. (1971). Recursive state estimation for a set-membership description of uncertainty. In *Automatic Control, IEEE Transactions on*, pages 117–128.

Gavrilets, V. (2003). *Aerobatic maneuvering of miniature helicopters*. Ph.D. Thesis.

Gavrilets, V., Mettler, B., and Feron, E. (2001). Nonlinear model for a small-size acrobatic helicopter. AIAA 4333.

Lefort, P. and Hamann, J. (1954). *L'hélicoptre théorie et pratique*. Chiron, 2e edition.

Mahony, R., Hamel, T., and Dzul, A. (1999). Hover control via approximate lyapunov control for a model helicopter. In *The confrence on Decision and Control*. Phoenix, Arizona, USA.

Maksarov, D. and Norton, J. (2002). Computationally efficient algorithms for state estimation with ellipsoidal approximations. International Journal of Adaptive Control and Signal Processing.

Milanese, M.and Norton, J., Piet-Lahanier, H., and Walter, E. (1996). *Bounding approaches to system identification*. Plenum Press, New York.

Murray, R., Li, Z., and Sastry, S. (1994). *A Mathematical Introduction to Robotic Manipulation*. CRC Press, Florida U.S.A.

Pronzato, L. and Walter, E. (1994). Minimal volume ellipsoids. In *International Journal Of Adaptative Control and Signal Processing*, pages 15–30.

Prouty, R. (1990). *Helicopter Performance, Stability and Control*. Robert E. Krieger, Malabar,Florida.

Schweppe, F. (1968). Recursive state estimation: Unknown but bounded errors and system inputs. In *IEEE Transactions on Automatic Control*, pages 22–28.